



Cite this: *J. Mater. Chem. B*, 2020, 8, 6798

Received 14th March 2020,  
Accepted 8th April 2020

DOI: 10.1039/d0tb00706d

rsc.li/materials-b

## Effect of molecular weight and polymer composition on gallol-functionalized underwater adhesive†

Jinhong Yu, Bohan Cheng and Hiroataka Ejima \*

Despite high demands from various industries, strong adhesion in a wet environment remains challenging. We investigated the underwater adhesion of gallol-functionalized polymers as a function of molecular weight and gallol content. By optimizing these parameters, the underwater adhesion strength of aluminium substrates exceeded 4 MPa. Therefore, the biomimetic molecular design of phenolic polymers is effective for the development of strong underwater adhesives.

Adhesives play an essential role in our daily life; however, commercial glues are usually designed only for use under dry conditions.<sup>1</sup> Under wet conditions, water forms an aqueous boundary layer between adhesives and adherents. This layer often makes the work of adhesion negative, which means underwater bonding is unfavourable.<sup>2</sup> In contrast, many marine creatures can stick to wet surfaces even under turbulent environments. A marine mussel is a well-studied animal owing to its wet adhesion ability. The key is the use of peculiar proteins with high 3,4-dihydroxyphenylalanine (DOPA) contents. The catechol group in DOPA plays a crucial role in adhesion,<sup>3</sup> which mediates various interactions, including hydrogen bondings,<sup>4</sup> metal coordinations,<sup>5,6</sup> cation- $\pi$  interactions,<sup>7</sup>  $\pi$ - $\pi$  interactions,<sup>8</sup> and covalent cross-linkings.<sup>9</sup> Among mussel-inspired adhesives,<sup>1,10–16</sup> poly(3,4-dihydroxystyrene-*co*-styrene) (P(VCat-*co*-St)) has shown the strongest adhesion strengths of 3.0 and 2.2 MPa in lap-shear and tensile tests, respectively, on aluminium substrates.<sup>16</sup>

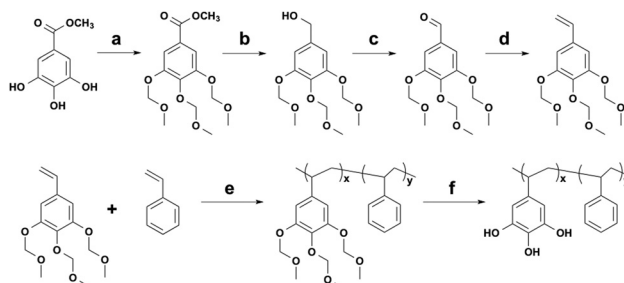
In addition to the catechol-based adhesives whose high underwater adhesion capabilities have been established, another phenolic compound, *viz.* gallol group, is recently gaining increasing attention.<sup>17,18</sup> As a member of the phenol family, gallol has three adjacent hydroxy groups attached to a benzene ring, and is often found in plant-derived polyphenols, including epigallocatechin<sup>19</sup> and tannic acid.<sup>20</sup> The gallol-functionalized copolymer, poly(3,4,5-trihydroxystyrene-*co*-*n*-butyl acrylate) (P(VGal-*co*-BA)) showed 7

times higher adhesion performance than its catechol-functionalized counterpart (P(VCat-*co*-BA)) under the same condition.<sup>21</sup> However, the adhesion strength of P(VGal-*co*-BA) was 1.0 MPa,<sup>21</sup> still lower than that of P(VCat-*co*-St).<sup>16</sup> This can be attributed to the different choice of comonomer (*i.e.*, BA and St).

Here, we first synthesized P(VGal-*co*-St) and investigated the effect of molecular weight and composition on the wet adhesion strength. Both tensile and lap-shear tests were carried out and the adhesion strength exceeded 4 MPa under the optimized conditions.

The synthesis of P(VGal *via* the methoxymethyl (MOM)-protection route was reported in our previous paper.<sup>21</sup> We slightly modified this protocol to start from the inexpensive compound, methyl gallate (Scheme 1 and Fig. S1, S2 in ESI†). We chose St as a comonomer because it may increase cohesive interactions *via*  $\pi$ - $\pi$  interactions. By changing the feed ratio of the initiator and monomer, the number-average molecular weight ( $M_n$ ) of the obtained polymer was controlled between 27 000 and 111 000 g mol<sup>-1</sup> (Table S1, ESI†).

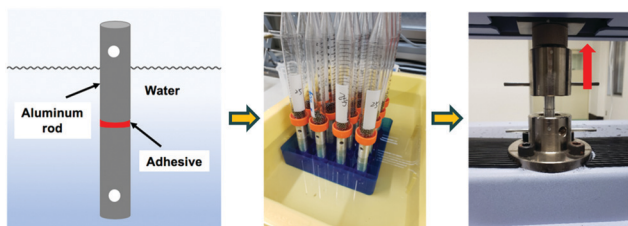
The underwater adhesion strength was measured using tensile and lap-shear geometries. In the tensile tests, a polished aluminium rod (1.27 cm in diameter and 38 cm in height) was completely submerged underwater (Scheme 2). The polymer



Scheme 1 Synthetic route of P(VGal-*co*-St). (a) DIEA, MOMCl, THF, 40 °C, 24 h. (b) LiAlH<sub>4</sub>, THF, 0 °C to r.t., 24 h. (c) MnO<sub>2</sub>, CH<sub>2</sub>Cl<sub>2</sub>, 24 h. (d) (Ph)<sub>3</sub>PCH<sub>3</sub>Br, *t*-BuOK, THF, 45 °C, 24 h. (e) AIBN, THF, 65 °C, 24 h. (f) HCl, MeOH, r.t., 24 h.

Department of Materials Engineering, School of Engineering, The University of Tokyo, 7-3-1 Hongo, Bunkyo-ku 113-8656, Japan. E-mail: ejima@material.t.u-tokyo.ac.jp

† Electronic supplementary information (ESI) available. See DOI: 10.1039/d0tb00706d



**Scheme 2** Experimental process for measuring underwater adhesion strength. The polymer solution was applied underwater and cured for a certain period. The samples were taken out from water and tested immediately.

solution ( $20 \mu\text{L}$ ,  $0.3 \text{ mg mL}^{-1}$ ) in a mixed solvent (chloroform : methanol = 9 : 1, v/v) was deposited on the rod by using a pipette. A second aluminium rod was placed atop the first rod. A weight ( $25 \text{ g}$ ) was placed on the second rod and incubated for a certain period for setting. Samples were then removed from water bath and tested on SHIMAZU AGS-X 10 kN load cell with a crosshead speed of  $10 \text{ mm min}^{-1}$ . The typical force–displacement curve is shown in Fig. S3 (ESI<sup>†</sup>). In the lap-shear test, aluminium plates ( $5 \text{ cm long} \times 1 \text{ cm wide}$ ) were used instead of the rods. The overlapped area of two plates was  $1 \text{ cm}^2$ .

The effect of setting time for underwater adhesion is shown in Fig. 1. For these experiments, we used P(VGal-co-St) with a fixed gallol content of  $\sim 10\%$  and varied  $M_n$  from  $27\,000$  to  $103\,000 \text{ g mol}^{-1}$ . As the solvent diffused out in a water bath, the chain mobility of the polymers decreased concomitantly. The polymer is finally glassified and set to bond the aluminium rods together. It took  $72 \text{ h}$  to reach its maximum adhesion strength, which is similar to the case of P(VCat-co-St).<sup>16</sup>

We then compared the adhesion strengths of polymers with different molecular weights (Fig. 2). In these tests, all the failure types were cohesive failures. This means that the adhesion between polymers and substrates is strong enough such that the adhesion strength is mainly determined by cohesive

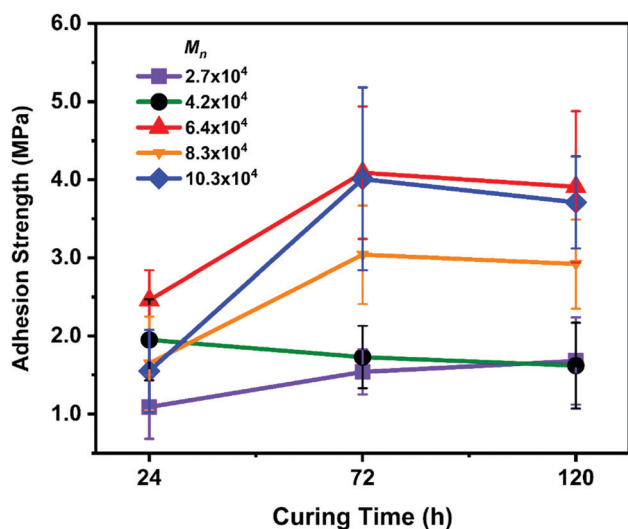


**Fig. 1** Adhesion strength with different curing times. Error bars indicate standard deviation,  $n \geq 5$ .

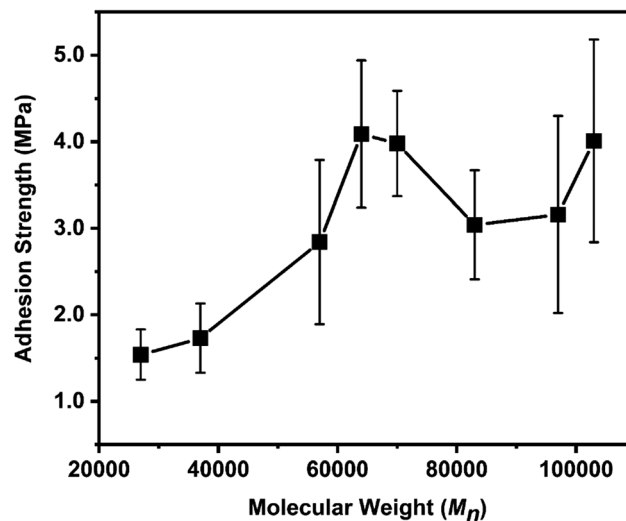


**Fig. 2** Adhesion strength as a function of number average molecular weight ( $M_n$ ). Error bars indicate standard deviation,  $n \geq 5$ .

interactions inside a polymer layer. In general, the properties of adhesives are highly dependent on the molecular weight and chemical composition.<sup>22,23</sup> In the regime of  $M_n < 64\,000 \text{ g mol}^{-1}$ , adhesion strength increased with increasing  $M_n$ . This is due to the increase in entanglement of polymer chains, considering that the entanglement molecular weight ( $M_e$ ) of PSt is  $\sim 17\,500 \text{ g mol}^{-1}$ .<sup>24</sup> Beyond  $64\,000 \text{ g mol}^{-1}$ , the bonding strength of this underwater adhesive reached its plateau. The highest adhesion strength was achieved at  $M_n = 64\,000$ , and the bonding strength was  $4.09 \pm 0.85 \text{ MPa}$  in tensile tests. Further increase in  $M_n$  did not lead to any significant increase in adhesion strength. The adhesion strength is affected by the complicated balance of polymer–surface (adhesive) and polymer–polymer (cohesive) interactions. Polymer with low  $M_n$  has high chain mobility, such that it can easily establish polymer–surface interactions; however, polymer–polymer interactions are weaker because the few entanglements and other interactions, including  $\pi$ – $\pi$  interactions and hydrogen bonding, exist between polymer chains. The low- $M_n$  polymer was quicker to set within  $24 \text{ h}$  (Fig. S4, ESI<sup>†</sup>), and the adhesion strength at the plateau region was weaker ( $\sim 1.2 \text{ MPa}$ ) than that for polymers with higher  $M_n$  ( $\sim 3$ – $4 \text{ MPa}$ ).

The adhesion strength of  $4.09 \pm 0.85 \text{ MPa}$  ( $M_n = 64\,000$ ) obtained in this study is nearly two times higher than that of catechol-based underwater adhesives ( $2.2 \text{ MPa}$ ).<sup>16</sup> The only difference is the number of phenolic hydroxy groups (*i.e.*, three for gallol and two for catechol). The underwater adhesion strength of P(VGal-co-St) with optimized  $M_n$  was also measured to be  $4.17 \pm 0.47 \text{ MPa}$  by using the lap-shear tests. This value is higher than that of P(VCat-co-St) ( $3.0 \text{ MPa}$ ),<sup>16</sup> suggesting that the gallol group is more effective than catechol for developing strong underwater adhesives.

Next, the effect of gallol content on adhesion strength was examined (Fig. 3). The polymer with 0% gallol content (PSt) has quite weak underwater adhesion, and usually fails during the tests. Interestingly, introducing a small amount of gallol groups ( $\sim 5\%$ ) dramatically enhanced the adhesion strength, which

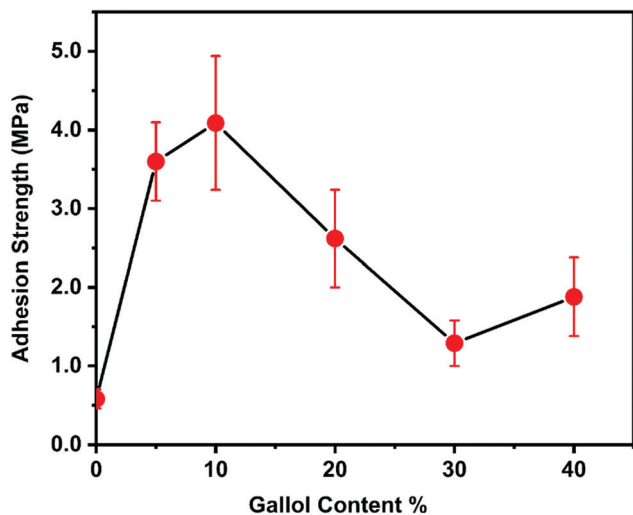


Fig. 3 Effect of gallol content on underwater adhesion strength. The error bars indicate standard deviation,  $n \geq 5$ .

exceeded 4 MPa at 10% gallol content. In contrast, increasing the gallol content beyond 10% decreased the adhesion strength. This might be partly because the gallol groups interacted with each other *via* hydrogen bonding and the number of free gallol groups, which can participate in the gallol-surface interactions, decreased.

Similar to catechol groups, gallol groups are susceptible to oxidation.<sup>17,19</sup> After the adhesion tests, the fractured samples were subjected to X-ray photoelectron spectroscopy (XPS) analysis. The  $C_{1s}$  spectrum of the fractured surface (10% gallol content,  $M_n = 64\,000\text{ g mol}^{-1}$ ) is shown in Fig. 4. The oxidation of gallol group forms quinone species, which increases the number of C=O bonds. By comparing C-O and C=O peak intensities, we estimated the oxidation degree of P(VGal<sub>10%</sub>-co-St<sub>90%</sub>). The peak areas of C-O and C=O accounted for 41.4% and 2.9%, respectively. Thus, ~7% of hydroxy groups were estimated to be oxidized after 72 h curing in water. It is noted that the oxidation degree of fresh polymer before curing

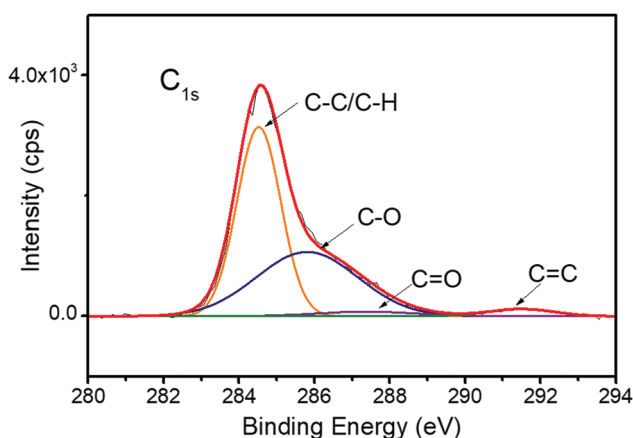


Fig. 4 XPS spectrum of P(VGal<sub>10%</sub>-co-St<sub>90%</sub>) remained on fractured surface after adhesion tests.

underwater was 0.2% (Fig. S5, ESI<sup>†</sup>). This low degree of oxidation ensured that the remaining adhesives were still soluble in organic solvents like acetone. The low gallol content (~10%), low oxidation degree (~7%), and high  $M_n$  (~64 000  $\text{g mol}^{-1}$ ) ensured good balance between adhesive and cohesive interactions in the polymer.

In summary, we synthesized the gallol-functionalized copolymers, P(VGal-co-St), with different  $M_n$  and compositions. The effects of curing time,  $M_n$ , and gallol content on the underwater adhesion strength were investigated in detail by using tensile and lap shear tests. With increasing molecular weight, the adhesion strength increased when  $M_n$  was less than 64 000. The introduction of ~10% gallol units is sufficient to achieve high adhesion strength. Under the optimized conditions, the underwater adhesion strength reached  $4.09 \pm 0.85$  MPa. This study demonstrates that the biomimetic molecular design of phenolic polymers focusing on the number of hydroxy groups is effective for developing strong underwater adhesive systems.

## Conflicts of interest

There are no conflicts to declare.

## Acknowledgements

This research was partially supported by the Japan Society for the Promotion of Science (JSPS) through KAKENHI Grant Numbers 18K14000, Adaptable and Seamless Technology transfer Program through Target-driven R&D (A-STEP) from Japan Science and Technology Agency (JST), and the Ogasawara Foundation for the Promotion of Science & Engineering. H. E. acknowledges JSPS for its Leading Initiative for Excellent Young Researchers.

## Notes and references

- 1 Y. Zhao, Y. Wu, L. Wang, M. Zhang, X. Chen, M. Liu, J. Fan, J. Liu, F. Zhou and Z. Wang, *Nat. Commun.*, 2017, **8**, 2218.
- 2 B. P. Lee, P. B. Messersmith, J. N. Israelachvili and J. H. Waite, *Annu. Rev. Mater. Res.*, 2011, **41**, 99–132.
- 3 H. Lee, N. F. Scherer and P. B. Messersmith, *Proc. Natl. Acad. Sci. U. S. A.*, 2006, **103**, 12999–13003.
- 4 S.-C. Li, J. Wang, P. Jacobson, X.-Q. Gong, A. Selloni and U. Diebold, *J. Am. Chem. Soc.*, 2009, **131**, 980–984.
- 5 T. Zhang, P. Wojtal, O. Rubel and I. Zhitomirsky, *RSC Adv.*, 2015, **5**, 106877.
- 6 M. Krosgaard, M. A. Behrens, J. S. Pedersen and H. Birkedal, *Biomacromolecules*, 2013, **14**, 297–301.
- 7 D. S. Hwang, H. Zeng, Q. Lu, J. Israelachvili and J. H. Waite, *Soft Matter*, 2012, **8**, 5640–5648.
- 8 J. Saiz-Poseu, J. Mancebo-Aracil, F. Nador, F. Busqué and D. Ruiz-Molina, *Angew. Chem., Int. Ed.*, 2019, **58**, 696–714.
- 9 J. Yang, M. A. Cohen Stuart and M. Kamperman, *Chem. Soc. Rev.*, 2014, **43**, 8271–8298.
- 10 M. Yu and T. J. Deming, *Macromolecules*, 1998, **31**, 4739–4745.

- 11 T. H. Anderson, J. Yu, A. Estrada, M. U. Hammer, J. H. Waite and J. N. Israelachvili, *Adv. Funct. Mater.*, 2010, **20**, 4196–4205.
- 12 C. R. Matos-Pérez, J. D. White and J. J. Wilker, *J. Am. Chem. Soc.*, 2012, **134**, 9498–9505.
- 13 L. Han, X. Lu, K. Liu, K. Wang, L. Fang, L.-T. Weng, H. Zhang, Y. Tang, F. Ren, C. Zhao, G. Sun, R. Liang and Z. Li, *ACS Nano*, 2017, **11**, 2561–2574.
- 14 Z. Guo, S. Mi and W. Sun, *J. Mater. Chem. B*, 2018, **6**, 6234–6244.
- 15 S. Yan, W. Wang, X. Li, J. Ren, W. Yun, K. Zhang, G. Li and J. Yin, *J. Mater. Chem. B*, 2018, **6**, 6377–6390.
- 16 M. A. North, C. A. Del Grosso and J. J. Wilker, *ACS Appl. Mater. Interfaces*, 2017, **9**, 7866–7872.
- 17 M. Shin, E. Park and H. Lee, *Adv. Funct. Mater.*, 2019, **29**, 1903022.
- 18 B. Cheng, K. Ishihara and H. Ejima, *Polym. Chem.*, 2020, **11**, 249–253.
- 19 K. Zhan, H. Ejima and N. Yoshie, *ACS Sustainable Chem. Eng.*, 2016, **4**, 3857–3863.
- 20 T. S. Sileika, D. G. Barrett, R. Zhang, K. H. A. Lau and P. B. Messersmith, *Angew. Chem., Int. Ed.*, 2013, **52**, 10766–10770.
- 21 K. Zhan, C. Kim, K. Sung, H. Ejima and N. Yoshie, *Biomacromolecules*, 2017, **18**, 2959–2966.
- 22 C. L. Jenkins, H. J. Meredith and J. J. Wilker, *ACS Appl. Mater. Interfaces*, 2013, **5**, 5091–5096.
- 23 G. Y. Choi, W. Zurawsky and A. Ulman, *Langmuir*, 1999, **15**, 8447–8450.
- 24 M. Kapnistos, M. Lang, D. Vlassopoulos, W. Pyckhout-Hintzen, D. Richter, D. Cho, T. Chang and M. Rubinstein, *Nat. Mater.*, 2008, **7**, 997–1002.